Clinical Cancer Research

Akt Inhibitors MK-2206 and Nelfinavir Overcome mTOR Inhibitor Resistance in Diffuse Large B-cell Lymphoma

Adam M. Petrich, Violetta Leshchenko, Pei-Yu Kuo, et al.

Updated Version	Access the most recent version of this article at: doi:10.1158/1078-0432.CCR-11-1407
Supplementary Material	Access the most recent supplemental material at: http://clincancerres.aacrjournals.org/content/suppl/2012/02/14/1078-0432.CCR-11-1407.DC1.html

Cited Articles	This article cites 39 articles, 18 of which you can access for free at: http://clincancerres.aacrjournals.org/content/18/9/2534.full.html#ref-list-1

E-mail alerts	Sign up to receive free email-alerts related to this article or journal.
Reprints and Subscriptions	To order reprints of this article or to subscribe to the journal, contact the AACR Publications Department at pubs@aacr.org.
Permissions	To request permission to re-use all or part of this article, contact the AACR Publications Department at permissions@aacr.org.

Cancer Therapy: Preclinical

Akt Inhibitors MK-2206 and Nelfinavir Overcome mTOR Inhibitor Resistance in Diffuse Large B-cell Lymphoma

Adam M. Petrich[1,2], Violetta Leshchenko[2], Pei-Yu Kuo[2], Bing Xia[2], Venu K. Thirukonda[1,2], Netha Ulahannan[2], Shanisha Gordon[2], Melissa J. Fazzari[2], B. Hilda Ye[2], Joseph A. Sparano[1,2], and Samir Parekh[1,2]

Abstract

Purpose: The mTOR pathway is constitutively activated in diffuse large B-cell lymphoma (DLBCL). mTOR inhibitors have activity in DLBCL, although response rates remain low. We evaluated DLBCL cell lines with differential resistance to the mTOR inhibitor rapamycin: (i) to identify gene expression profile(s) (GEP) associated with resistance to rapamycin, (ii) to understand mechanisms of rapamycin resistance, and (iii) to identify compounds likely to synergize with mTOR inhibitor.

Experimental Design: We sought to identify a GEP of mTOR inhibitor resistance by stratification of eight DLBCL cell lines with respect to response to rapamycin. Then, using pathway analysis and connectivity mapping, we sought targets likely accounting for this resistance and compounds likely to overcome it. We then evaluated two compounds thus identified for their potential to synergize with rapamycin in DLBCL and confirmed mechanisms of activity with standard immunoassays.

Results: We identified a GEP capable of reliably distinguishing rapamycin-resistant from rapamycin-sensitive DLBCL cell lines. Pathway analysis identified Akt as central to the differentially expressed gene network. Connectivity mapping identified compounds targeting Akt as having a high likelihood of reversing the GEP associated with mTOR inhibitor resistance. Nelfinavir and MK-2206, chosen for their Akt-inhibitory properties, yielded synergistic inhibition of cell viability in combination with rapamycin in DLBCL cell lines, and potently inhibited phosphorylation of Akt and downstream targets of activated mTOR.

Conclusions: GEP identifies DLBCL subsets resistant to mTOR inhibitor therapy. Combined targeting of mTOR and Akt suppresses activation of key components of the Akt/mTOR pathway and results in synergistic cytotoxicity. These findings are readily adaptable to clinical trials. *Clin Cancer Res; 18(9); 2534–44. ©2012 AACR.*

Introduction

Diffuse large B-cell lymphoma (DLBCL) is the most common subtype of non–Hodgkin lymphoma (NHL). Approximately 30% of patients relapse and die of these aggressive tumors despite chemotherapy and stem cell transplant (1). Therefore, new treatment approaches for DLBCL are urgently needed.

The mTOR pathway is constitutively activated in NHL, and mTOR inhibition has emerged as a potential therapeutic option for solid tumors, especially renal cell carcinoma

(RCC; ref. 2), and the NHL subtypes mantle cell lymphoma (MCL; ref. 3) and DLBCL (4). Rapamycin, the prototypical mTOR inhibitor, binds to the immunophilin FKBP and inhibits cell-cycle progression by blocking cytokine-mediated signal transduction pathways. This interrupts downstream signals that regulate gene expression, cellular metabolism, and apoptosis (5). However, response rates to mTOR inhibitors remain approximately 30% in DLBCL (6, 7). Mechanisms of resistance to mTOR inhibition are poorly understood (3, 7). Gene expression profiling (GEP) is an important tool to recognize genes and pathways responsible for resistance to chemotherapeutic agents (8). To date, GEP has not only been helpful in the delineation of prognostically important subtypes of DLBCL, but also in identifying potentially important targets and therapies (9).

We sought to identify and explore in a preclinical model the gene expression signature associated with differences in resistance to rapamycin in DLBCL. This gene signature proved to be an accurate biomarker for predicting response to rapamycin in DLBCL cell lines. Because differentially expressed genes associated with resistance to rapamycin are enriched for the Akt pathway, we investigated the potential for Akt inhibitors to augment the antilymphoma

Authors' Affiliations: [1]Montefiore Medical Center; and [2]Albert Einstein College of Medicine, Bronx, New York

Current address for A.M. Petrich: Division of Hematology/Oncology, Feinberg School of Medicine, Northwestern University, Chicago, IL.

Corresponding Author: Samir Parekh, Albert Einstein College of Medicine, 111 East 210th Street Bronx, NY 10467. Phone: 718-920-4826; Fax: 718-798-7474; E-mail: sparekh@montefiore.org

Translational Relevance

There is a large unmet need for advances in the treatment of relapsed and refractory diffuse large B-cell lymphoma (DLBCL). Recent trials of mTOR inhibitors in this population have shown low response rates, and mechanisms of resistance are poorly described for these drugs. We have identified a gene expression signature that proved to be an accurate biomarker for predicting response to rapamycin in DLBCL cell lines. Using a systems biology approach consisting of pathway analysis and connectivity mapping, we next identified Akt inhibitors MK-2206 and nelfinavir capable of overcoming resistance to rapamycin. These findings create a basis for combining these agents with rapamycin in clinical trials for patients with lymphoma and support the use of gene expression profiles for patient selection for mTOR inhibitor therapy.

effect of rapamycin. We specifically tested nelfinavir, a protease inhibitor (PI) used in the treatment of human immunodeficiency virus (HIV) infection, and MK-2206, an orally bioavailable compound currently in early-phase trials in patients with solid tumors. Our results show synergism between Akt inhibitors and rapamycin in reduction of DLBCL cell viability, inhibition of downstream genes in the Akt pathway, and interruption of feedback between mTOR inhibition and Akt.

Materials and Methods

Cell lines, culture conditions, and drug treatment

DLBCL cell lines Farage, Karpas-422, OCI-Ly1, OCI-Ly3, OCI-Ly18, OCI-Ly19, Pfeiffer, SUDHL-4, SUDHL-6, SUDHL-8, Toledo, and WSU-NHL, and breast cancer cell lines MDA-MB 231 and MDA-MB 468, were each cultured in RPMI-1640 medium (CellGro) supplemented with 10% FBS (Gemini Bio-Products), 2 mmol/L L-glutamine, 100 U/mL penicillin G, and 100 μg/mL streptomycin (CellGro), at 37°C with humidification. Rapamycin was purchased from Sigma Aldrich, MK-2206 from Selleck Chemicals, and vinblastine from Calbiochem. Each drug was formulated at stock solutions between 200 nmol/L and 1 μmol/L. Doxorubicin was obtained from Teva Pharmaceuticals and formulated at 500 nmol/L. Purified nelfinavir was a generous gift from Pfizer and was formulated at 200 μmol/L, after dissolution in dimethyl sulfoxide (DMSO). All drugs were stored at between −20 and −88°C. Cells were treated in series of 8 100 μL wells for 48 hours for viability assessment, and in 4 mL wells in triplicate, for 24 hours, for flow cytometry and to determine protein amounts.

Cell viability assay

Cell viability was determined by a fluorometric resazurin reduction method (CellTiter-Blue; Promega) following the manufacturer's instructions. The number of viable cells in each treated well was calculated 48 hours after treatment. Cells (100 μL; 10^5 cells per well for lymphoma cell lines and 4×10^3 cells per well for breast cancer cell lines) were plated in 96-well plates (8 replicates per condition), with 20 μL of CellTiter-Blue reagent (Promega) added to each well. After 1 hour of incubation with the dye (2 hours for breast cancer cell lines), fluorescence (560 Ex/590 Em) was measured with the Polarstar Optima microplate reader (BMG Lab Technologies). The number of viable cells in each treated well was calculated on the basis of the linear least squares regression of the standard curve. Cell viability in drug-treated cells was normalized to their respective untreated controls. Cell counts were confirmed on the Countess automated cell counter (Invitrogen) according to the manufacturer's specifications.

Gene expression arrays and analysis

Gene expression data were obtained using the Affymetrix HuGene ST 1.0 GeneChip; mRNA isolation, labeling, hybridization, and quality control were carried out as described previously (10). Raw data were processed with the Robust Multi-array Averaging (RMA) algorithm and Affymetrix Expression Console software. Data are available in the NCBI Gene Expression Omnibus (GEO) database (accession number GSE27255; National Center for Biotechnology Information, Gene Expression Omnibus database; http://ncbi.nlm.nih.gov/geo). A total of 33,297 probes were measured on the array. The association between gene expression and cell line resistance was assessed first using a conventional t test and second with a modified t test used by the eBayes function in limma (R version 9.2; refs. 11, 12). The final set of candidates was defined as those genes differentially expressed between resistant and sensitive cell lines with a P value, by both methods, below 0.03. This cutoff value was chosen to provide a reasonably sized set of genes that was felt likely to retain predictive power. Pathway Analysis was conducted using Ingenuity (www.ingenuity.com/products/pathways_analysis.html). In this program, the core analysis function was selected, and default analysis settings were maintained (direct and indirect relationships; maximum 35 molecules per network; maximum 25 networks per analysis), with the exception of cell lines, which were limited to lymphoma.

To predict resistance patterns of additional cell lines not included in the training set (see Results first section), the collection of genes was analyzed using the support vector machine (SVM) prediction module from Gene Pattern software (http://www.broadinstitute.org/cancer/software/genepattern/). An SVM (with linear kernel) uses all gene expression values as input and fits a classifying line, with the largest margin separating the 2 classes (resistant vs. sensitive cell lines), in this feature space, which has as many dimensions as the number of genes submitted. This classifying line, also called a hyperplane, is then used to classify each unknown cell line (in our case as either "sensitive" or "resistant") based upon which side of the hyperplane each test case falls.

The GEP data were then analyzed with the Broad Institute's Connectivity Map (cmap) database (http://www.broadinstitute.org/cmap/index.jsp), using the same set of differentially expressed genes in resistant versus sensitive

cell lines. With cmap, our imported query was compared with established signatures of therapeutic compounds (or "perturbagens"). Each compound was assigned a connectivity score (from +1 to −1), representing relative association with our specific query. Compounds with connectivity scores closest to −1 were considered most likely capable of reversing the gene pattern of our query (i.e., overcoming resistance), and were therefore considered the best candidates for functional validation in an attempt to confer rapamycin sensitivity.

The online database Oncomine (www.oncomine.org/resource/login.html) was then used to evaluate Akt expression in primary tissue samples. In Oncomine, data sets are composed of samples represented as microarray data measuring either mRNA expression or DNA copy number on primary tumors, cell lines, or xenografts, generally from published research. These data sets include sample metadata, which is used to set up analyses on groups of interest (cancer vs. normal, etc). These data sets are collected from public repositories, such as GEO and Array Express, and by communicating with study authors, and permit searching for specific disease types, tissue types, and/or genes. Our search was conducted using the filters Akt (gene name) and lymphoma (disease type).

Cell-cycle analysis

Approximately 10^6 cells of each cell line were harvested (along with untreated controls) after 12 hours of treatment in 12-well plates. Cells were washed with PBS and resuspended in 400 μL of solution containing propidium iodide and RNase. Cell cycle was analyzed with a Becton-Dickinson Flow Cytometer, and proportional cell-cycle distribution was assessed with ModFit software.

Protein estimation by luminex assay

Approximately 2×10^6 cells were treated (along with untreated controls) for 3 and 6 hours in 12-well plates. Cells were lysed with radioimmunoprecipitation assay (RIPA) buffer. A commercially available multiplex panel (Millipore) was used to analyze proteins in the PI3K/Akt/mTOR pathway using the manufacturer's recommended technique. Colored bead sets, each of which was coated by the manufacturer with a specific capture antibody, were introduced into 200 μL wells (96-well plates) containing approximately 30 μg of protein. After the sample analyte was captured by the bead, a biotinylated detection antibody was introduced. The mixture was then incubated with streptavidin–phycoerythrin (PE) conjugate, the reporter molecule, to complete the reaction on the surface of each bead. The beads were passed through dual laser excitation (Luminex 100 Flow Cytometer) for identification and quantification. The data were analyzed with the Luminex LDS Flow Cytometry Software (v 1.7), with all values calculated as a proportion of glyceraldehyde-3-phosphate dehydrogenase (GAPDH).

Western blot analysis

After treatment, cells were harvested and washed with ice-cold PBS, and subsequently lysed with RIPA buffer with fresh PIs. Total protein concentrations were estimated by the Lowry method. Approximately 30 μg of each sample was resolved on Tris-glycine gels made in our laboratory, with 15% acrylamide for 4-EBP-1, and 10% acrylamide for all other proteins. These were transferred to nitrocellulose filters, which were incubated overnight at 4°C with rabbit antibodies against phosphorylated S6 ribosomal protein (p-S6RP; Ser 235/236; 1:1,000), phosphorylated 4-EBP-1 (p-4-EBP-1; Thr 37/46, 1:1,000), phosphorylated Akt (p-Akt; Ser473; 1:250), total Akt (1:250), caspase-3 (1:500), and PARP (1:500; all antibodies obtained from Cell Signaling Technology). Secondary antibodies (goat anti-rabbit), were incubated for at least 1 hour at room temperature. Actin was measured with a conjugated horseradish peroxidase (HRP) antibody. Western blotting luminol reagent (Santa Cruz Biotechnology) was subsequently applied and the membranes were exposed to film for between 10 seconds and 1 hour. Blot patterns were analyzed with ImageJ software (http://rsbweb.nih.gov/ij/), providing a quantitative measure of protein expression.

Assessment of synergy

All determinations of synergism were made with Calcusyn Software (Biosoft), based upon the mathematical equations of Chou and Talalay (13). Degrees of synergism are expressed as combination indices (CI), with smallest values indicating the most synergy. CI values less than 0.8 indicate synergy; those 0.8 to 1.2 indicate an additive effect; and those more than 1.2 indicate antagonism.
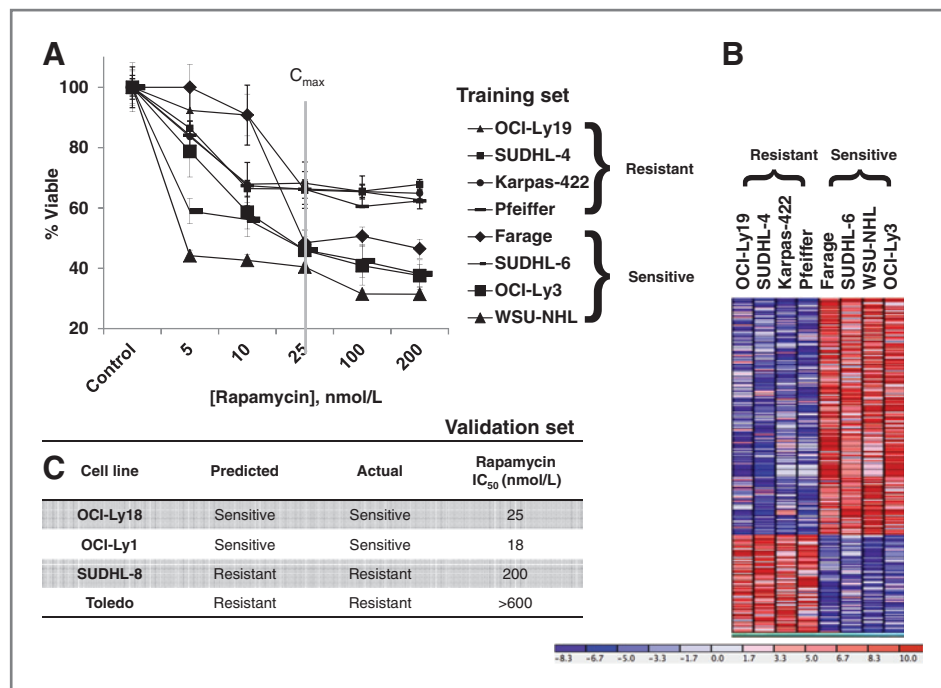
Results

Gene expression profiling identifies a signature capable of predicting rapamycin resistance in 6 DLBCL cell lines

Eight germinal center B-cell (GCB) DLBCL cell lines were treated with rapamycin in the dose range of 5 to 200 nmol/L (see Fig. 1A), based upon therapeutically achievable concentrations (14, 15). In our experiments, rapamycin decreased cell viability by approximately 30% to 60% in the 8 cell lines examined and resulted in stratification into 2 groups: 4 cell lines (SUDHL-6, Farage, OCI-Ly3, and WSU-NHL) with IC_{50} value at 25 nmol/L or lower and the other 4 (SUDHL-4, OCI-Ly19, and Karpas-422, and Pfeiffer) with IC_{50} value of greater than 200 nmol/L (Fig. 1A). The majority of the cell lines (6 of 8) have a doubling time between 30 to 40 hours (16, 17). Accounting for the doubling time of the resistant cell line Karpas (60–90 hours; ref. 16), and sensitive cell line OCI-Ly3 (24 hours; ref. 18), would not change their stratification in our system. We were able to therefore classify these cell lines into 2 groups based on fluorometric resazurin reduction assay results (see Materials and Methods) as a surrogate for cell viability.

Global gene expression was measured in the cell lines by the Affymetrix HuGene ST 1.0 Arrays. A heatmap representing the 239 significantly (P value < 0.03) differentially expressed genes between resistant and sensitive cell lines is shown in Fig. 1B. We next examined a multivariable model for resistance based on expression using a linear

Figure 1. Gene expression profiling identifies a signature capable of predicting rapamycin resistance in DLBCL cell lines. A, a total of 10^6 DLBCL cells per mL were treated with rapamycin, 5 to 200 nmol/L for 48 hours. DLBCL cell lines corresponding to the dose-response curves are labeled to the right of the figure, in order of degree of resistance. These cell lines comprised the "training" set of our pattern recognition algorithm. The posttreatment cell viability was evaluated by a fluorometric resazurin reduction assay. The x-axis depicts rapamycin concentration; the y-axis, the percentage of viable cells as compared with control. The values of each point represent the mean ± SD derived from octuplicate measurements. This was conducted three times for each cell line, with representative results shown. The C_{max} in patients with cancer, as derived from a phase I trial (15), is indicated by the gray vertical line. B, using both conventional and modified t test (see Materials and Methods), a signature of those genes differentially expressed between rapamycin-sensitive and rapamycin-resistant cell lines, with significance of $P < 0.03$ was identified. This signature is represented here by a supervised clustering heatmap, as generated by the GenePattern Server. C, the signature shown in (B) was analyzed with the SVM class prediction algorithm found on the GenePattern Server to predict response patterns of 6 additional cell lines (composing our validation set). The predicted and observed response patterns of those cell lines, along with corresponding IC_{50} levels, are shown.

SVM (see Materials and Methods) and the 239 top univariate candidates. We found that the resistance patterns of 4 additional DLBCL cell lines, whose IC_{50} concentrations we determined experimentally, were accurately predicted by our SVM-based classifier (Fig. 1C).

## Gene expression profiles of rapamycin response of DLBCL cell lines identify central role for Akt

To identify pathways and functional groups enriched by differentially expressed loci, our 239-gene signature ($P < 0.03$) was evaluated with the Ingenuity Pathway Analysis (IPA) database core analysis module (see Materials and Methods). The most enriched network identified (network score = 26, with network functions hematological system development and function, humoral immune response, and tissue morphology) revolved around the serine threonine kinase Akt (Fig. 2A). The top 2 biologic functions identified by the core analysis were cancer (the Fisher exact test P value 1.33×10^{-3}–4.3×10^{-2}, with 27 molecules identified) and hematologic disease (the Fisher exact test P value 1.33×10^{-3}–3.71×10^{-2}, with 10 molecules identified; see Fig. 2B). When the GEP signature was narrowed to include only those genes significantly overexpressed in

resistant cell lines, Akt maintained a central position in the most enriched pathway (Supplementary Fig. S1A).

We then examined Akt expression in healthy ($n = 6$) and malignant ($n = 56$) primary (human) lymphoid tissue samples using the Oncomine database to determine Akt expression in primary NHLs. The data set resulting from our query (as described in Materials and Methods) provided normalized expression values of Akt for activated B-cell–like DLBCL (ABC-DLBCL; $n = 26$); germinal cell B-cell–like DLBCL (GCB-DLBCL; $n = 30$); and normal B cells ($n = 6$), each derived from a study describing GEPs characteristic of GCB- and ABC-DLBCL (19). Akt mRNA was relatively overexpressed in DLBCL as compared with normal lymphoid tissue, with approximately two thirds of all samples showing relative overexpression of this gene (Fig. 2C).

Higher p-Akt protein levels are associated with poor prognosis in DLBCL (20) and other malignancies (21), (22). We therefore asked the question whether Akt levels, as determined by Western blotting, would correlate with resistance to rapamycin in DLBCL cell lines. We found evidence of a loose correlation between total Akt and IC_{50} values for the 8 cell lines tested (Fig. 2D; source Western blotting shown in Supplementary Fig. S1B). However, we
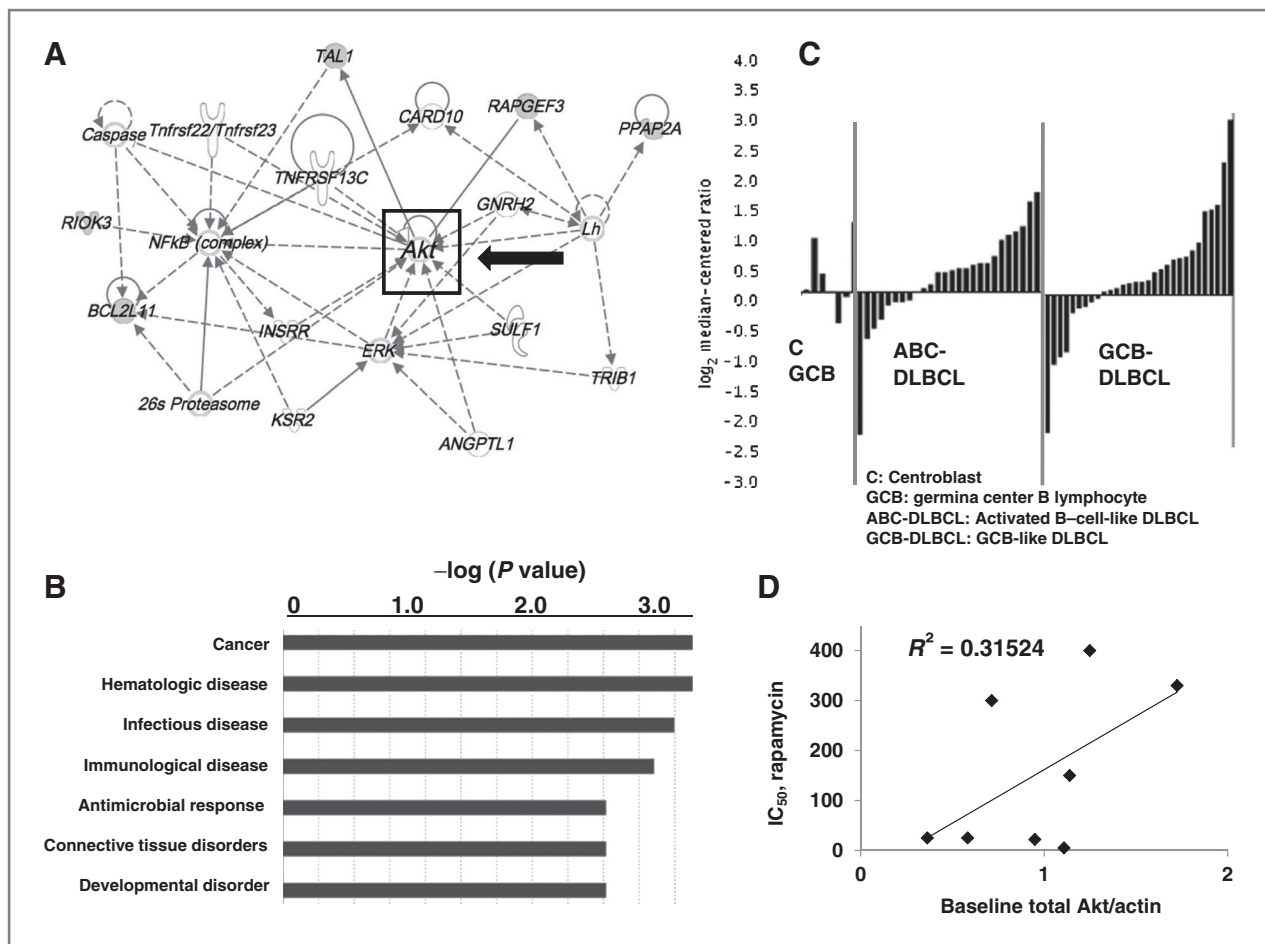
Figure 2. GEPs of rapamycin response of DLBCL cell lines identify central role for Akt. A and B, the signature shown in Fig. 1B was analyzed using the core analysis function on the IPA server. A diagram of the top network enriched by this analysis is shown (A). The most enriched biologic functions, as determined by IPA core analysis of the same signature, are shown in (B), with the Fisher exact test P values as shown. C, the Oncomine database was queried using gene name Akt1, using disease-type filter "lymphoma." This provided levels of Akt gene expression levels in healthy B cells (C, centroblast; GCB, germinal center B lymphocyte; $n = 6$), activated B-cell–like DLBCL (ABC-DLBCL; $n = 26$), and GCB-like DLBCL (GCB-DLBCL; $n = 30$) samples of primary (human) tissue samples. These data are represented here as a waterfall plot for each set of samples, in which the y-axis represents $\log_2$ median-centered ratio, and each sample is displayed in order of this ratio value. D, protein levels of total Akt and actin were assayed by Western blotting. Levels of total Akt were quantified as compared with actin (x-axis; measured with ImageJ as described in Materials and Methods) and then plotted against the IC_{50} value (y-axis) for that particular cell line.

also found that higher levels of p-Akt (Supplementary Fig. S1C), including as a proportion of total Akt (Supplementary Fig. S1D), inversely correlated with IC_{50} values, such that sensitive cell lines had overall higher levels of p-Akt.

Connectivity mapping identifies Akt inhibitors that synergize with rapamycin at clinically relevant doses

In light of (i) the relatively low response rates of patients with DLBCL seen in trials of mTOR inhibitors (6, 7) and (ii) the fact that data mining of gene expression profiles can identify novel drugs capable of overcoming chemotherapy resistance (23), we next sought to use GEP data for *in silico* identification of drugs most likely to overcome resistance to mTOR inhibitors. Connectivity mapping of differentially expressed genes between rapamycin-sensitive and -resistant cell lines (see Materials and Methods), provided a ranked

list of candidate compounds in order of likelihood of efficacy for reversing the GEP-associated resistance. In this list, 2 phosphoinositide 3-kinase (PI3K) inhibitors (wortmannin and LY294002), the PI saquinavir, and multiple histone deacetylase (HDAC) inhibitors (including both vorinostat and trichostatin-A), were all identified within the top 2% of the candidate compounds (Fig. 3A).

While PI3K and HDAC inhibition have been previously described to synergize with mTOR inhibitors (24, 25), we reasoned that inhibition of Akt would represent a novel strategy to augment therapeutic activity of mTOR inhibition in DLBCL. We elected to investigate Akt inhibition with 2 agents: MK-2206, a highly selective allosteric inhibitor of Akt; and nelfinavir, a PI used frequently for treatment of HIV. MK-2206 was chosen for its target specificity, and because there are safety and efficacy data in humans
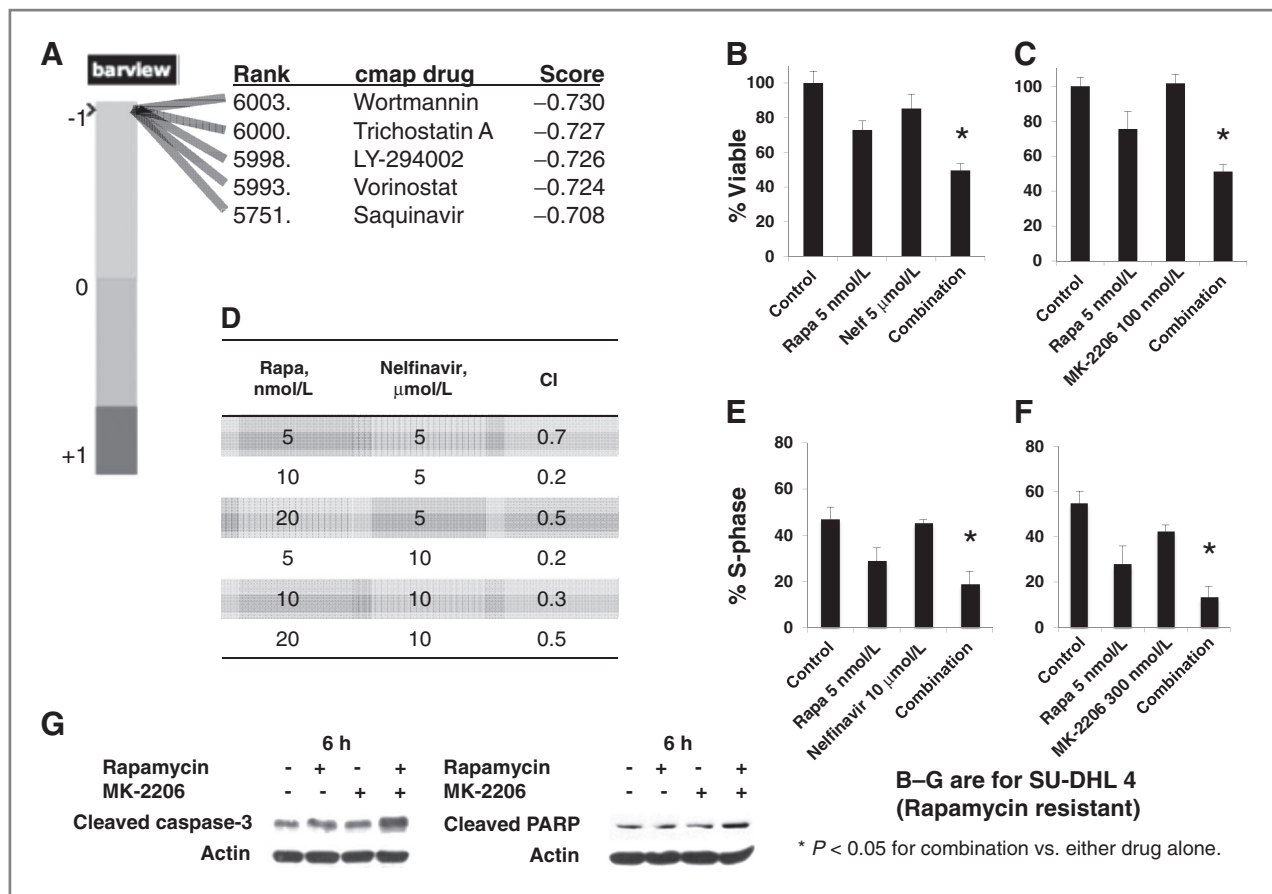
Figure 3. Connectivity mapping can identify compounds targeting the PI3K/Akt pathway, which synergize with rapamycin at clinically relevant doses. A, the signature of differentially expressed genes was submitted for analysis to the connectivity map (cmap) server. Shown here are the rank, name, and cmap score of selected compounds, each within the top 2% of perturbagens, as determined by analysis of this signature. B and C, a total of 10^6 cells per mL of 2 rapamycin-sensitive cell lines (SUDHL-6 and WSU-NHL) and 2 rapamycin-resistant cell lines (SUDHL-4 and OCI-Ly19) were treated with rapamycin, an Akt inhibitor (either nelfinavir or MK-2206), and the combination of rapamycin and an Akt inhibitor, for 48 hours. Viability was assessed by a fluorometric resazurin reduction assay. Each experiment was carried out in octuplicate, and repeated twice, with representative results shown. Viability patterns of the rapamycin-resistant cell line SUDHL-4 treated with rapamycin (Rapa) and nelfinavir (Nelf; B), and rapamycin and MK-2206 (C), are shown. The y-axis represents percentage of cells viable. D, CI values were calculated using the Chou–Talalay equation, as used by Calcusyn software, for the 4 cell lines described earlier (SUDHL-6, WSU-NHL, SUDHL-4 and OCI-Ly19). Shown here are the CI values observed in the SUDHL-4 cell line. Similar results, indicative of synergy, were achieved in the other 3 cell lines. E and F, a total of 10^6 cells per mL of the same 4 DLBCL cell lines (SUDHL-6, WSU-NHL, SUDHL-4, and OCI-Ly19) were treated for 12 hours with rapamycin and nelfinavir (Nelf; E), and rapamycin and MK-2206 (F), and then analyzed by flow cytometry after staining with propidium iodide. Each experiment was repeated twice under independent conditions, with representative results shown. The proportion of cells in each treatment group found to be in S-phase is shown as a marker of cell-cycle progression. The y-axis represents percentage of cells in S-phase. G, rapamycin-resistant cell lines (SUDHL-4 and OCI-Ly19) were treated for 6 hours with rapamycin at 25 nmol/L, MK-2206 at 300 nmol/L, and the combination, after which cell lysates were prepared and analyzed by Western blot technique. Each experiment was repeated, with representative results provided. Shown here are results from analysis of cleaved caspase-3 (left) and cleaved PARP (right), in the SUDHL-4 cell line.

(26). Nelfinavir was chosen because (i) of preclinical evidence showing that it inhibits activity of Akt (27); (ii) it has the most potent antitumor activity among its class of drug (including saquinivir; ref. 28); (iii) as an U.S. Food and Drug Administration (FDA)-approved medication, it has ample pharmacokinetic, pharmacodynamic (PK/PD), and safety data. We compared the synergy (with rapamycin) in antilymphoma effects between the specific Akt inhibitor MK-2206, and the PI nelfinavir, which likely inhibits Akt through an indirect mechanism (27), by assaying cell viability, cell-cycle changes, and inhibition of downstream genes in the Akt/mTOR pathway in DLBCL cell lines. We also studied the effect of combining rapamycin with MK-2206 on the viability of 2 breast cancer cell lines, MDA-MB 231 and MDA-MB-468, to help determine whether the combination effects were specific to lymphoma cell lines. Then, to help validate the predictive accuracy of connectivity mapping, we sought a commonly used cytotoxic chemotherapeutic agent predicted by our connectivity mapping results to be unlikely to overcome rapamycin resistance. In this manner, we identified the agent vinblastine, a microtubule disruptive agent used in lymphoid malignancies and solid tumors, for further testing in combination with rapamycin.

We found that rapamycin showed synergistic effects with nelfinavir in inhibiting cell viability in rapamycin-resistant cell lines (SUDHL-4, Fig. 3B) as well as rapamycin-sensitive cell lines (SUDHL-6, Supplementary Fig. SA2). CI values less than 1 were shown in 4 cell lines tested [SUDHL-4 (shown in Fig. 3D), SUDHL-6, OCI-Ly19, and WSU-NHL]. Rapamycin also showed synergistic effects on cell viability when used with MK-2206 (Fig. 3C). CI values less than 1 were again shown for each cell line (SUDHL-4, SUDHL-6, OCI-Ly19, and WSU-NHL) when treated with rapamycin and MK-2206 (Supplementary Fig. S2B). Taken together, our data indicate that rapamycin synergizes effectively with both nelfinavir and MK-2206 in a panel of 4 DLBCL cell lines, including 2 (SUDHL-4 and OCI-Ly19) that we previously classified as resistant to rapamycin as a single agent (see Fig. 1A). Significant synergy was observed with combining rapamycin and MK-2206 in breast cancer cell lines (Supplementary Fig. S5), suggesting that the therapeutic effects of dual targeting of mTOR and Akt are not limited to lymphoma cell lines. We also found that the combinations of rapamycin with vinblastine in SUDHL 4 and SUDHL 6 cell lines were not synergistic, and in fact antagonistic, with CI values more than 1 (Supplementary Fig. S6), suggesting that connectivity mapping can predict for both the presence and absence of synergism.

To investigate the mechanism of synergy, we next examined effects of these agents on cell cycle and apoptosis. To evaluate cell-cycle effects, cells were treated with individual agents and combinations, then analyzed for cell-cycle phase distributions by flow cytometry (see Materials and Methods). The combinations of rapamycin and nelfinavir, and rapamycin and MK-2206, produced greater reduction in proportion of cells in S-phase than when any single drug was used alone. This phenomenon was shown in both rapamycin-resistant cell lines (Fig. 3E and F; Supplementary Fig. S2C and S2D) and rapamycin-sensitive cell lines (Supplementary Fig. S2E and S2F). We next evaluated caspase-3 and PARP cleavage as markers of apoptosis. We found that, in SUDHL-4 cells, levels of cleaved forms of both proteins were increased by the combination of rapamycin and MK-2206 as compared with control and/or either drug alone (Fig. 3G). Nelfinavir also increased the levels of cleaved caspase-3 and PARP compared with control, although these levels were not further decreased in the combination of rapamycin and nelfinavir (Supplementary Fig. S3A).

Akt activation is induced by rapamycin treatment; this activation is abrogated by Akt inhibitors

In light of data suggesting that rapamycin treatment can induce Akt phosphorylation via a TORC2-mediated feedback mechanism in DLBCL (24), we examined whether this phenomenon could be abrogated in DLBCL cell lines by Akt inhibitors MK-2206 and nelfinavir. Using a flow cytometric–based multiplex assay for Akt/mTOR pathway proteins, we found increased p-Akt levels in the rapamycin-sensitive cell line SUDHL-6, but not in the rapamycin-resistant cell line SUDHL-4, after short exposure to rapamycin (Fig. 4A). Furthermore, the use of either nelfinavir or

MK-2206 decreased levels of p-Akt, even in the presence of rapamycin, particularly after 6 hours of exposure (Fig. 4A and B).

We sought to confirm these findings with immunoblotting, and indeed found that rapamycin induced Akt activation in rapamycin-sensitive cell lines (though not clearly in rapamycin-resistant cell lines), and that the combination of rapamycin with either MK-2206 (Fig. 4C and D; Supplementary Fig. S3B and S3C) or nelfinavir (Supplementary Fig. S4A–C) led to a significant decrease in the levels of p-Akt relative to rapamycin treatment alone. Importantly, neither nelfinavir nor MK-2206 negatively affected rapamycin-induced inhibition of phosphorylation of mTOR targets S6RP and translational cofactor 4-EBP-1.

mTOR inhibition and Akt inhibition synergize with cytotoxic chemotherapy in DLBCL

We next asked the question whether mTOR inhibitors and Akt inhibitors would synergize with chemotherapy used in DLBCL. To do so, we evaluated the effects of doxorubicin, a potent cytotoxic antilymphoma agent, in combination with rapamycin and MK-2206. Using each agent at concentrations achievable in humans, with treatment for 48 hours, we found that both rapamycin and MK-2206 synergize with doxorubicin in reduction of cell viability (Supplementary Fig. S7A and S7B). The 3 drug CIs for doxorubicin, rapamycin, and MK-2206 were well below 0.8, signifying mathematical confirmation of synergy (Supplementary Fig. S7C) in all 4 cell lines studied [SUDHL-4 and OCI-Ly19 (rapamycin resistant); SUDHL-6 and WSU-NHL (rapamycin sensitive)].

Discussion

In summary, we show here that gene expression profiling has the ability to predict resistance to rapamycin, in which the expression of Akt is central. We subsequently identify agents that inhibit Akt and synergize with the mTOR inhibitor rapamycin in reduction of viability, inhibition of cell-cycle progression, and promotion of apoptosis. Our data suggest that simultaneous mTOR and Akt inhibition is an effective strategy to substantiate rapamycin cytotoxicity in both rapamycin-sensitive and -resistant DLBCL cell lines.

Gene expression signatures that subclassify DLBCL and predict response to chemoimmunotherapy have been described (29). The accurate stratification of cell line responses to rapamycin by GEP supports further testing of these signatures in future clinical trials of mTOR inhibitors in DLBCL. Notably, cDNA-mediated annealing, selection, extension, and ligation (DASL) technology (30, 31) may allow use of paraffin-embedded tissues to obtain genomic expression data, which would circumvent the need to obtain fresh frozen samples from patients. We believe that our data represents a framework for a technique that could offer early and precise prediction of response to mTOR inhibitors and should permit better selection of patients for treatment using these agents.

After confirming that connectivity mapping could positively predict for the presence of synergy, we felt it was
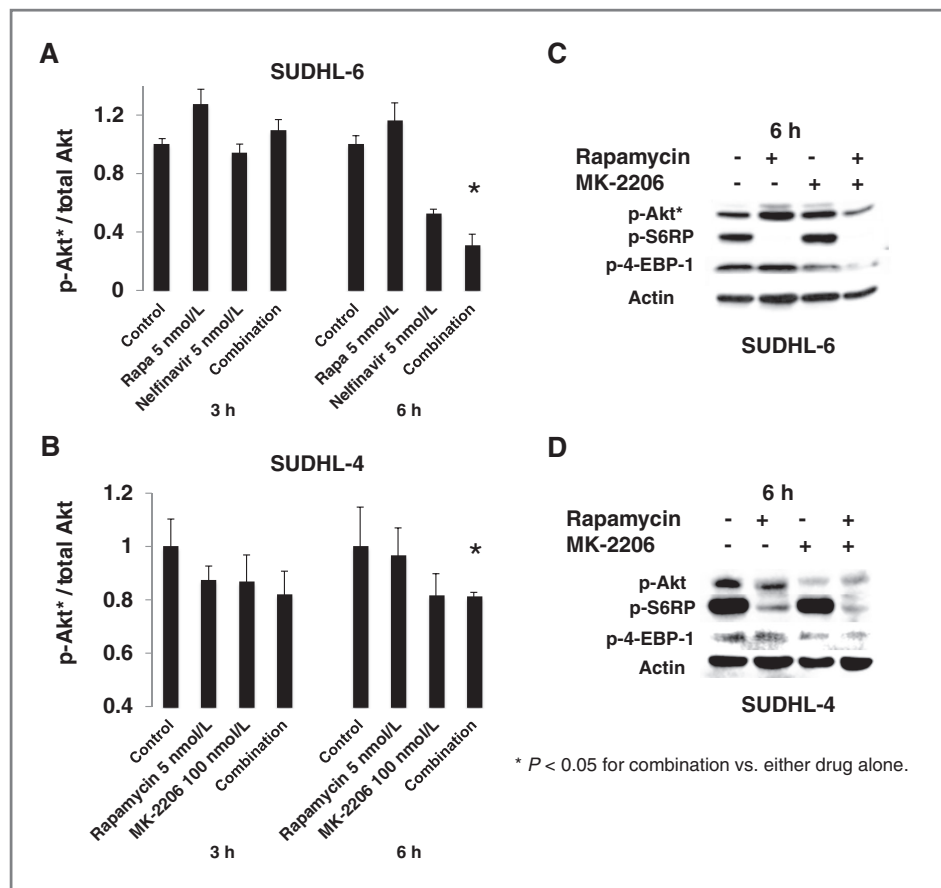
Figure 4. Akt activation is induced by rapamycin treatment, and Akt inhibitors abrogate rapamycin-induced Akt activation. A and B, a total of 10^6 cells per mL of the same 4 DLBCL cell lines (SUDHL-6, WSU-NHL, SUDHL-4, and OCI-Ly19) were treated with rapamycin, an Akt inhibitor (either nelfinavir or MK-2206), and the combination of rapamycin and Akt inhibitor for 3 and 6 hours. A flow cytometric–based multiplex protein assay of p-Akt, as a proportion of total Akt, was conducted in SUDHL-6 (rapamycin sensitive) cells treated with rapamycin and nelfinavir (A) and SU-DHL 4 (rapamycin resistant) cells treated with rapamycin and MK-2206 (B). Each experiment was carried out in triplicate, in independent conditions, with mean and SD displayed. *, statistically significant differences (P value < 0.05; t test). C and D, one rapamycin-resistant cell line (SUDHL-4) and one rapamycin-sensitive cell line (SUDHL-6) were treated for 6 hours with rapamycin (25 nmol/L), nelfinavir (15 μmol/L), and the combination; or rapamycin (25 nmol/L), MK-2206 (300 nmol/L), and the combination; after which cell lysates were prepared and analyzed by Western blot technique. Each experiment was repeated, with representative results provided. Shown here are results from analysis of p-Akt, p-S6RP, and p-4-EBP-1 in SUDHL-6 cells (C) and SUDHL-4 cells (D) treated with rapamycin (5 nmol/L) and MK-2206 (100 nmol/L) for 6 hours.

warranted to determine whether it could predict the opposite (i.e., for the lack of synergy). We therefore identified vinblastine as an agent predicted not to have synergistic properties with rapamycin and experimentally showed antagonistic effects upon cell viability. Similar results were obtained for metformin, another pharmacologic agent predicted to be devoid of synergistic effect when combined with rapamycin (data not shown).

High levels of tissue Akt phosphorylation have been associated with inferior clinical outcomes in breast cancer (21), lung cancer (22), and DLBCL (20), though none of these studies included patients treated with mTOR inhibitors. Some authors have associated increased Akt activation with increased sensitivity to mTOR inhibition (32–34), and our data showing increased p-Akt in sensitive cell lines would certainly support this. However, others have observed mTOR inhibitor resistance in tumors with PI3K/Akt activation: in a phase I trial of patients with PTEN

(phosphatase and tensin homolog deleted on chromosome 10)-deficient glioblastoma treated with rapamycin, baseline Akt upregulation was associated with a significantly shorter time to progression (35). Taken together, these data indicate that the ability of p-Akt levels to predict mTOR inhibitor resistance might be tumor dependent and should be further investigated in future trials.

Other recent preclinical and clinical findings support the idea that inhibiting proteins upstream or downstream of mTOR in the PI3K/Akt/mTOR pathway can overcome mTOR inhibitor resistance. Simultaneous Akt/PI3K and mTOR inhibition by the novel agent NVP-BEZ235 showed nanomolar efficacy in rapamycin-resistant primary effusion lymphoma cell lines (36); and the Akt/PI3K inhibitor LY294002 was efficacious in multiple DLBCL cell lines. In this study, however, elevated p-Akt levels predicted for increased resistance to LY294002, suggesting that targeting of both Akt and PI3K might allow for the greatest

therapeutic efficacy. Gupta and colleagues showed that p-Akt was upregulated by mTOR inhibitor treatment in DLBCL cell lines and patients and that treatment with HDAC inhibition overcame this effect and synergized with mTOR inhibition (24). In our experiments, treatment of DLBCL cells with rapamycin alone did not produce apoptosis, consistent with the results reported by Wanner and colleagues (37). However, the baseline cleavage of caspase-3 and PARP was significantly increased upon combination of the Akt inhibitors. Our data support a novel strategy for inhibition of the PI3K/Akt/mTOR pathway by synergistic application of Akt inhibitors, along with rapamycin, the prototypical mTOR inhibitor. In addition, our data indicates that the phosphorylation of Akt is a dynamic and reactive process in DLBCL and can be modulated with therapeutic benefit by the use of Akt inhibitors.

We chose to target Akt with MK-2206, as it has been shown to inhibit activation of all 3 isoforms of Akt at nanomolar doses and synergize with cytotoxic and targeted chemotherapy agents in preclinical models (38). Based upon preclinical data and xenograft models, MK-2206 is known to be highly selective for Akt1 and Akt2 over other members of the AGC family of kinases, inhibition of which required MK-2206 concentrations more than 50 μmol/L (39). We therefore believe that all concentrations of MK-2206 used in our experimentation would have maintained a high level of specificity for Akt, and that desired pharmacologic effects were primarily due to Akt inhibition, as opposed to off-target effects. Most importantly, MK-2206 has shown safety and efficacy in early-phase human trials (26). We believe that the demonstration of synergism between rapamycin and MK-2206 is a significant step in its optimal deployment in future clinical trials.

PIs, a class of antiretroviral agents used widely in the treatment of HIV and acquired immunodeficiency syndrome (AIDS), have been shown to effectively downregulate Akt phosphorylation by inhibiting proteasome activity and inducing the unfolded protein response, which in turn leads to a global decrease in protein synthesis (14). Nelfinavir, a PI that is FDA approved for use in HIV/AIDS, can sensitize malignant cells to both chemotherapy (40) and radiation (41). Of 6 clinically relevant PIs tested in the NCI-60 panel of cancer cell lines, nelfinavir showed the most potent effects in decreasing viability of this panel of cancer cell lines (28). It has also been noted that the PI3K/Akt pathway is upregulated in HIV-related malignancies associated with Epstein–Barr virus (EBV) and Kaposi sarcoma herpes virus (KSHV; ref. 42), and this has formed the rationale for successful testing of inhibitors of the PI3K/Akt/mTOR pathway in preclinical models of these tumors (36). The lifetime incidence of NHL is dramatically increased in patients with HIV/AIDS and DLBCLs comprise the vast majority of histologic subtypes of these AIDS-related lymphomas (ARL; ref. 43). Patients with HIV/AIDS are widely excluded from participation in clinical trials of antineoplastic agents, and data for the optimal treatment of ARL are therefore lacking. Advances in the safe and effective treatment of ARL, including therapy aimed at HIV itself, are

therefore urgently needed. We believe that our data, showing the presence and mechanism of synergy between nelfinavir and rapamycin, support the potential for nelfinavir to be used in clinical trials for the treatment of ARL, and perhaps other AIDS-related malignancies as well. Because both rapamycin and nelfinavir are FDA-approved compounds, their use is supported by significant safety and efficacy data, and repositioning them as antineoplastic agents (alone or in combination) is significantly faster than bringing new compounds to market (15). Likewise, safety data for the use of MK-2206 in humans are already reported, facilitating its investigation in clinical trials, particularly as compared with other compounds yet to be tested beyond the laboratory.

Our data suggest that exposure to the mTOR inhibitor rapamycin seemed to upregulate expression of p-Akt in sensitive cell lines, but not necessarily in resistant cell lines. This is consistent with the notion that mTOR inhibitors induce greater perturbation of cellular function in sensitive cell lines than resistant cell lines. But this also suggests that resistant cell lines may have additional mechanisms of resistance to mTOR inhibition, which is unlikely to be explained simply by studying levels of one isoform of p-Akt. Rather, resistance may be related to either qualitative differences in p-Akt (e.g., phosphorylation at sites other than serine 473), or variation in the quantity or quality of other molecules in the Akt/mTOR pathway, which would only be captured with wider pathway-based or genomic studies (such as of our 239-gene profile). Regardless of the actual explanation for these observed differences, we view the *in silico* identification of agents that can ultimately synergize with rapamycin, in both rapamycin-sensitive and rapamycin-resistant cell lines, to be an important finding of this work.

In conclusion, our results identify a GEP-based signature for predicting response to rapamycin in DLBCL and support Akt inhibition as a viable strategy for producing synergistic antilymphoma cytotoxicity with mTOR inhibition. More broadly, our approach supports the use of global RNA expression and drug discovery using connectivity mapping to identify synergistic drug combinations for cancer therapy and to improve the selection of appropriate patients.

References

1. Sehn LH, Berry B, Chhanabhai M, Fitzgerald C, Gill K, Hoskins P, et al. The revised International Prognostic Index (R-IPI) is a better predictor of outcome than the standard IPI for patients with diffuse large B-cell lymphoma treated with R-CHOP. Blood 2007;109: 1857–61.
2. Hudes G, Carducci M, Tomczak P, Dutcher J, Figlin R, Kapoor A, et al. Temsirolimus, interferon alfa, or both for advanced renal-cell carcinoma. N Engl J Med 2007;356:2271–81.
3. Hess G, Herbrecht R, Romaguera J, Verhoef G, Crump M, Gisselbrecht C, et al. Phase III study to evaluate temsirolimus compared with investigator's choice therapy for the treatment of relapsed or refractory mantle cell lymphoma. J Clin Oncol 2009; 27:3822–9.
4. Hess G, Smith SM, Berkenblit A, Coiffier B. Temsirolimus in mantle cell lymphoma and other non-Hodgkin lymphoma subtypes. Semin Oncol 2009;36 Suppl 3:S37–45.
5. Sehgal SN. Rapamune (Sirolimus, rapamycin): an overview and mechanism of action. Therapeutic Drug Monitoring 1995;17: 660–5.
6. Smith SM, van Besien K, Karrison T, Dancey J, McLaughlin P, Younes A, et al. Temsirolimus has activity in non-mantle cell non-Hodgkin's lymphoma subtypes: The University of Chicago phase II consortium. J Clin Oncol 2010;28:4740–6.
7. Witzig TE, Reeder CB, Laplant BR, Gupta M, Johnston PB, Micallef IN, et al. A phase II trial of the oral mTOR inhibitor everolimus in relapsed aggressive lymphoma. Leukemia 2011;25:341–7.
8. Riedel RF, Porrello A, Pontzer E, Chenette EJ, Hsu DS, Balakumaran B, et al. A genomic approach to identify molecular pathways associated with chemotherapy resistance. Mol Cancer Ther 2008;7: 3141–9.
9. Iqbal J, Liu Z, Deffenbacher K, Chan WC. Gene expression profiling in lymphoma diagnosis and management. Best Pract Res Clin Haematol 2009;22:191–210.
10. Rosenwald A, Wright G, Wiestner A, Chan WC, Connors JM, Campo E, et al. The proliferation gene expression signature is a quantitative integrator of oncogenic events that predicts survival in mantle cell lymphoma. Cancer Cell 2003;3:185–97.
11. Smyth G. Linear models and empirical Bayes methods for assessing differential expression in microarray experiments. Stat Appl Genet Mol Biol 2004;3:1–26.
12. Smyth GK. Limma: linear models for microarray data. In:Gentleman R, Carey V, Dudoit S, Irizarry R, Huber W, editors. Bioinformatics and computational biology solutions using R and bioconductor. New York: Springer; 2005. p. 397–420.
13. Chou TC, Talalay P. Quantitative analysis of dose-effect relationships: the combined effects of multiple drugs or enzyme inhibitors. Adv Enzyme Regul 1984;22:27–55.
14. Zimmerman JJ, Kahan BD. Pharmacokinetics of sirolimus in stable renal transplant patients after multiple oral dose administration. J Clin Pharmacol 1997;37:405–15.
15. Jimeno A, Rudek MA, Kulesza P, Ma WW, Wheelhouse J, Howard A, et al. Pharmacodynamic-guided modified continuous reassessment method-based, dose-finding study of rapamycin in adult patients with solid tumors. J Clin Oncol 2008;26:4172–9.
16. DSMZ. [cited 2011 May 30]. Available from: http://www.dsmz.de/ human_and_animal_cell_lines/.
17. ATCC. [cited 2011 May 30]. Available from: http://www.atcc.org/.
18. Tweeddale ME, Lim B, Jamal N, Robinson J, Zalcberg J, Lockwood G, et al. The presence of clonogenic cells in high-grade malignant lymphoma: a prognostic factor. Blood 1987;69: 1307–14.
19. Alizadeh AA, Eisen MB, Davis RE, Ma C, Lossos IS, Rosenwald A, et al. Distinct types of diffuse large B-cell lymphoma identified by gene expression profiling. Nature 2000;403:503–11.
20. Uddin S, Hussain AR, Siraj AK, Manogaran PS, Al-Jomah NA, Moorji A, et al. Role of phosphatidylinositol 3′-kinase/AKT pathway in diffuse large B-cell lymphoma survival. Blood 2006;108: 4178–86.
21. Zhou X, Tan M, Stone Hawthorne V, Klos KS, Lan K-H, Yang Y, et al. Activation of the Akt/mammalian target of rapamycin/4E-BP1 pathway by ErbB2 overexpression predicts tumor progression in breast cancers. Clin Cancer Res 2004;10:6779–88.
22. David O, Jett J, LeBeau H, Dy G, Hughes J, Friedman M, et al. Phospho-Akt overexpression in non-small cell lung cancer confers significant stage-independent survival disadvantage. Clin Cancer Res 2004;10:6865–71.
23. Lamb J, Crawford ED, Peck D, Modell JW, Blat IC, Wrobel MJ, et al. The Connectivity Map: using gene-expression signatures to connect small molecules, genes, and disease. Science 2006;313: 1929–35.
24. Gupta M, Ansell SM, Novak AJ, Kumar S, Kaufmann SH, Witzig TE. Inhibition of histone deacetylase overcomes rapamycin-mediated resistance in diffuse large B-cell lymphoma by inhibiting Akt signaling through mTORC2. Blood 2009;114:2926–35.
25. Sos ML, Fischer S, Ullrich R, Peifer M, Heuckmann JM, Koker M, et al. Identifying genotype-dependent efficacy of single and combined PI3K- and MAPK-pathway inhibition in cancer. Proc Natl Acad Sci U S A 2009;106:18351–6.
26. Tolcher AW, Yap I, Fearen A. A phase I study of MK-2206, an oral potent allosteric Akt inhibitor (Akti), in patients (pts) with advanced solid tumor (ST). J Clin Oncol 27:15s, 2009 (suppl; abstr 3503).
27. Gupta AK, Li B, Cerniglia GJ, Ahmed MS, Hahn SM, Maity A. The HIV protease inhibitor nelfinavir downregulates Akt phosphorylation by inhibiting proteasomal activity and inducing the unfolded protein response. Neoplasia 2007;9:271–8.
28. Gills JJ, Lopiccolo J, Tsurutani J, Shoemaker RH, Best CJM, Abu-Asab MS, et al. Nelfinavir, A lead HIV protease inhibitor, is a broad-spectrum, anticancer agent that induces endoplasmic reticulum stress, autophagy, and apoptosis in vitro and in vivo. Clin Cancer Res 2007;13: 5183–94.
29. Lenz G, Wright G, Dave SS, Xiao W, Powell J, Zhao H, et al. Stromal gene signatures in large-B-cell lymphomas. N Engl J Med 2008; 359:2313–23.
30. Abramovitz M, Ordanic-Kodani M, Wang Y, Li Z, Catzavelos C, Bouzyk M, et al. Optimization of RNA extraction from FFPE tissues for expression profiling in the DASL assay. Biotechniques 2008; 44:417–23.
31. April C, Klotzle B, Royce T, Wickham-Garcia E, Boyaniwsky T, Izzo J, et al. Whole-genome gene expression profiling of formalin-fixed, paraffin-embedded tissue samples. PLoS One 2009;4:e8162.
32. Macaskill EJ, Bartlett JM, Sabine VS, Faratian D, Renshaw L, White S, et al. The mammalian target of rapamycin inhibitor everolimus (RAD001) in early breast cancer: results of a pre-operative study. Breast Cancer Res Treat 2011;128:725–34.
33. Wendel HG, De Stanchina E, Fridman JS, Malina A, Ray S, Kogan S, et al. Survival signalling by Akt and eIF4E in oncogenesis and cancer therapy. Nature 2004;428:332–7.
34. Beeram M, Tan Q-TN, Tekmal RR, Russell D, Middleton A, DeGraffenried LA. Akt-induced endocrine therapy resistance is reversed by inhibition of mTOR signaling. Ann Oncol 2007;18:1323–8.
35. Cloughesy TF, Yoshimoto K, Nghiemphu P, Brown K, Dang J, Zhu S, et al. Antitumor activity of rapamycin in a Phase I trial for patients with recurrent PTEN-deficient glioblastoma. PLoS Med 2008;5:e8.
36. Bhatt AP, Bhende PM, Sin S-H, Roy D, Dittmer DP, Damania B. Dual inhibition of PI3K and mTOR inhibits autocrine and paracrine proliferative loops in PI3K/Akt/mTOR-addicted lymphomas. Blood 2010;115: 4455–63.
37. Wanner K, Hipp S, Oelsner M, Ringshausen I, Bogner C, Peschel C, et al. Mammalian target of rapamycin inhibition induces cell cycle arrest in diffuse large B cell lymphoma (DLBCL) cells and sensitises DLBCL cells to rituximab. Br J Haematol 2006;134: 475–84.
38. Hirai H, Sootome H, Nakatsuru Y, Miyama K, Taguchi S, Tsujioka K, et al. MK-2206, an allosteric Akt inhibitor, enhances anti-tumor efficacy by standard chemotherapeutic agents or

molecular targeted drugs *in vitro* and *in vivo*. Mol Cancer Ther 2010;9:1956–67.

39. Bilodeau MT, Balitza AE, Hoffman JM, Manley PJ, Barnett SF, Defeo-Jones D, et al. Allosteric inhibitors of Akt1 and Akt2: a naphthyridinone with efficacy in an A2780 tumor xenograft model. Bioorg Med Chem Lett 2008;18:3178–82.

40. Yang Y, Ikezoe T, Nishioka C, Bandobashi K, Takeuchi T, Adachi Y, et al. NFV, an HIV-1 protease inhibitor, induces growth arrest, reduced Akt signalling, apoptosis and docetaxel sensitisation in NSCLC cell lines. Br J Cancer 2006;95:1653–62.

41. Plastaras JP, Vapiwala N, Ahmed MS, Gudonis D, Cerniglia GJ, Feldman MD, et al. Validation and toxicity of PI3K/Akt pathway inhibition by HIV protease inhibitors in humans. Cancer Biol Ther 2008;7:628–35.

42. Damania B. Targeting the PI3K/Akt/mTOR pathway in AIDS-associated malignancies. In: Dittmer DP, Krown SE, editors. Molecular basis for therapy of AIDS-defining cancers. New York: Springer; 2010. p. 152–66.

43. Navarro WH, Kaplan LD. AIDS-related lymphoproliferative disease. Blood 2006;107:13–20.